

SPINUA: A FLEXIBLE PROCESSING CHAIN FOR ERS / ENVISAT LONG TERM INTERFEROMETRY

F. Bovenga⁽¹⁾, R. Nutricato⁽¹⁾, A. Refice⁽²⁾, L. Guerriero⁽¹⁾, M. T. Chiaradia⁽¹⁾

⁽¹⁾ *Dipartimento Interateneo di Fisica, Via Amendola 173, 70126 Bari (Italy), E-mail: fabio.bovenga@ba.infn.it*

⁽²⁾ *ISSIA-CNR, Via Amendola 122/d, 70126 Bari (Italy), E-mail: refice@ba.issia.cnr.it*

ABSTRACT

The SPINUA (Stable Point INterferometry over Un-urbanised Areas) processing chain has been developed and tested in the framework of ASI-, ESA- and EU-funded projects, and represents an effort to adapt and optimise the general approach of long-term SAR interferometry for the study of un-urbanised areas such as those typical of Mediterranean sites affected by slope instabilities. In this work, the SPINUA processing framework is presented organically, highlighting innovative aspects and some ad hoc solutions which render the tool flexible and suitable for applications to areas characterized by low densities of persistent scatterers, of either spatially-extended or point-like nature. Examples of processing results are presented.

1. INTRODUCTION

Differential Interferometric SAR (DInSAR) techniques were able to give successful results on landslide sites close to urban areas [1] or located on rocky alpine glaciers [2]. However, other case studies reported in the recent literature [3], [4], [5], [6] indicate that several factors limit the practical applicability of the standard DInSAR technique to landslide monitoring. Coherence loss and atmospheric effects represent the most serious drawbacks.

Multi-temporal DInSAR provides a partial solution to the effects of atmospheric artefacts and coherence losses. In the past few years, several differential processing methodologies have been introduced and experimented on multi-temporal interferometric data with the aim of detecting long-term deformation. In particular, two main strategies can be distinguished:

- the Persistent Scatterers Interferometry (PSI) approach [7], which studies the phase information over single isolated objects characterised by a high temporal phase stability; this approach is usually implemented by computing differential interferograms of all the acquisitions w.r.t. to the same reference master image, then performing advanced phase analyses on the pixels exhibiting stable SAR response throughout the stack;
- other methods that exploit differential interferograms obtained from pairs of images with the best values of spatial baseline (e.g. below a certain threshold) and

then infer, through different procedures (LMS, SVD), the connected time series of phase values due to deformation [8], [9], [10].

The complicated aspect in both the above-mentioned approaches is the need of joint non-linear estimation of stochastic fields due to atmospheric signal, deformation, and errors in the reference DEM. Usually, the atmospheric phase screen delay signal is assumed to be totally uncorrelated in time but correlated in the space domain, with a spatial frequency spectrum which follows a power law [11]. Displacement fields, on the other hand, are expected to have certain correlation properties both in time and space, which depend on the particular case and type of application (e.g. subsidence, landslides, etc.). A reliable discrimination of the two above-mentioned types of contribution requires careful considerations of both signals' characteristics, such as typical spatial-temporal scales, etc.

Other considerations concern the pre-processing requirements, which are in some cases more stringent for the PSI approach than in the second class of algorithms. Moreover, the latter usually produce displacement maps at lower spatial resolution, and seem to be more susceptible to artefacts in presence of non-connected interferometric phase subsets [12].

The SPINUA (Stable Point INterferometry over Un-urbanised Areas) processing chain, which has been developed by the remote sensing group of Dipartimento Interateneo di Fisica – Politecnico di Bari and is being maintained and constantly upgraded jointly by the Dipartimento Interateneo di Fisica and the ISSIA-CNR of Bari in the framework of ASI, ESA and European projects, follows mainly the PSI strategy.

2. PROCESSING OUTLINE

The general PSI technique has been successfully applied to many test sites affected by terrain displacements such as subsidence, tectonic movements, and building collapse; all these case studies were conducted on sites mainly in or close to urban areas [13]. On such environmental conditions, in fact, persistent scatterer (PS) point density is usually high (of the order of 100 PS/km²), and very reliable results can be achieved (about 2-3 mm/year as displacement sensitivity). The situation changes in the case of un-urbanised areas. Problems in these cases can be classified in two types:

first, the objective scarcity of PS objects on the terrain; second, the difficulty of detection of existing PS on such sites.

The first problem is not specific only to landslides, but to all applications of the technique on areas characterized by low antropization. Although, for processes occurring at regional scale, the possibility of processing larger scenes may ease the problem, for the specific landslide case the typically small areas affected by the phenomenon, together with the fact that local variations in the atmospheric phase screen (APS) can be strong in high-topography regions, is a serious limit.

A possible way to deal with this first problem can be to enlarge the class of objects which can be detected and monitored through the technique. In this direction can be seen the recent efforts to expand the applicability of the method to multi-frequency and/or multi-angle acquisitions, and to integrate ascending and descending passes [14]. Also, investigations on the real nature of PS objects are of great relevance [15]. Another important possibility is that offered by techniques such as SAR polarimetry, to better characterize the scattering behaviour of point-like objects [16].

Although no definitive solution is still available, the above-mentioned problem can be at least mitigated by using ad hoc, optimized algorithms for e.g. interpolation and co-registration, aimed at minimizing both the influence of the background noise and the processing errors in the PS preliminary identification. For instance, an assessment has been carried out to choose the best oversampling factor and the best interpolation kernel given the number of available SAR acquisitions in the dataset and the a priori expected maximum phase noise power [17]. This approach is integrated into the SPINUA processing framework. Moreover, the critical processing step of co-registration for each image pair made of the single “master” and one of the several “slaves” can be split into several partial steps which exploit acquisitions separated by small temporal and geometric baselines. Each partial step is affected by a lower contribution of decorrelation noise with respect to the “single master” case. This approach has been theoretically cast in a minimum spanning tree framework, and it has been shown that several solutions can be adopted for the combination of SAR images into InSAR pairs, depending on the definition of a “distance” measure as a function of the expected co-registration quality [18]. Such stepwise approach allows to increase the number of detected Persistent Scatterer Candidates (PSCs) of up to 10% on landslide test datasets [19].

To deal with the second problem, more advanced processing has to be applied. Although the most recent reports on applications of the original PS technique adopt non-linear models for APS and also for displacement

contributions, the exact extent to which such methods can be applied is not completely clear. For example, the usually adopted model for the APS structure function is, as mentioned, a power law, with the exponent numerical value related to the typical spatial scale of atmospheric inhomogeneities. This model, originated by studies on atmospheric water vapor spatial statistics [20], was demonstrated by Hanssen on ERS SAR interferograms acquired over the Netherlands [21], and is used as a priori information in current PSI processing to infer the spatial autocorrelation properties of the APS, and thus separate the latter from the other contributions in the PS phase history. However, it is questionable that such model of the APS spatial structure can be assumed also on sites with strong topography. In such cases, indeed, the topographic contribution to the atmospheric spatial profile could be more important than the spatial inhomogeneities due to water vapor stochastic fluctuations. This is also supported by observations of variogram trends of APS components estimated on some test sites [22]. In these cases, estimation procedures based on the autocorrelation characteristics of APS data often fail, since the APS exhibits the same spatial structure as topography.

Another limit to the processing comes just from the degraded performances of APS, DEM error and velocity estimation in conditions of low density of PS benchmarks, even for the case of linear behaviour for all contributions. In fact, estimation procedures tend to get drowned in “statistical noise” when low redundancy is present in the data. Also, they are strongly influenced by phase aliasing phenomena, causing ambiguities.

Countermeasures for this latter type of problem adopted in the SPINUA approach include e.g. ad hoc sparse grid phase unwrapping algorithms [24], [25], which take into account the scaling properties of the atmospheric signal in order to drive the unwrapping procedure.

3. ALGORITHM PROCESSING STEPS

Fig. 1 shows in a schematic form the processing flow of the SPINUA technique. The system accepts in input single-look complex (SLC) SAR images in CEOS format, and a DEM of the area in UTM coordinates. The output products are shown in the yellow box. The intermediate products, consisting of the co-registered amplitude image stack and the differential interferogram stack, are also shown for completeness. In the following sections, each module is briefly described.

3.1 Input Data

The input SAR data are CEOS-formatted, standard SLC products. ENVISAT data must be all acquired with the same sensor configuration. In order to obtain final consistent information from both ERS and ENVISAT data, the latter must be acquired in Image Mode,

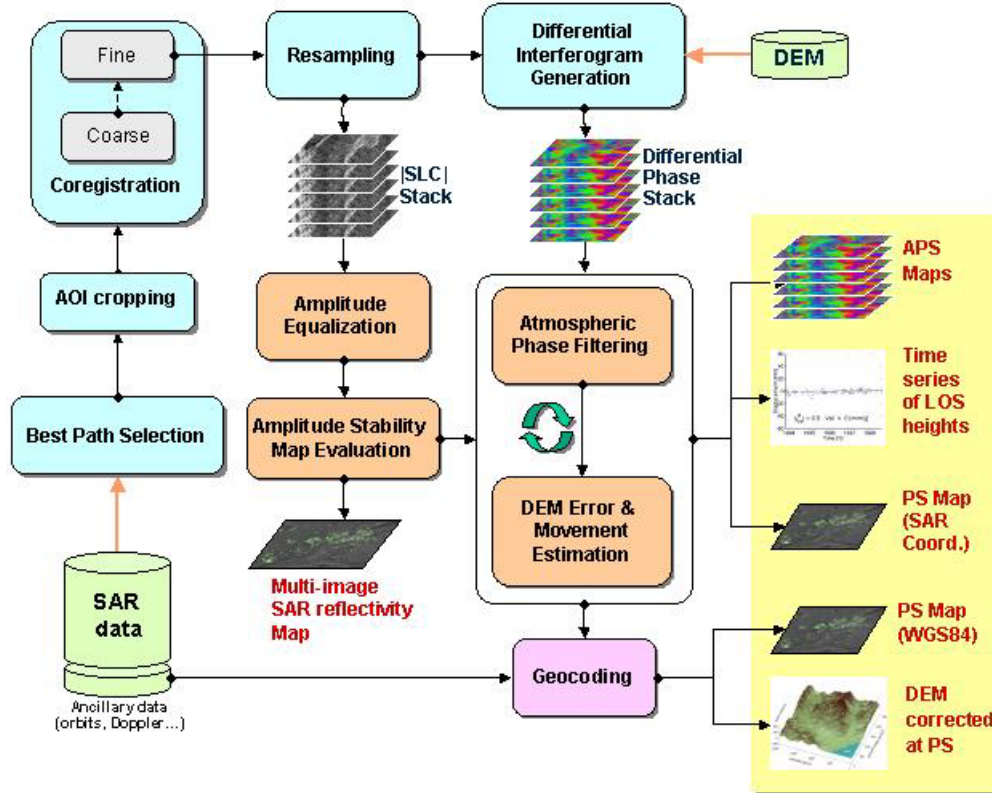


Fig. 1. Flow chart of the SPINUA processing methodology.

Swath 2.

3.2 AOI cropping

An area of interest (AOI) can be defined, by specifying row and column intervals on the master image geometry. Although the system can process whole ERS/ENVISAT frames, the selection of a sub-area speeds up considerably the whole processing chain. Considerations about the presence of man-made structures, and then the expected density and distribution of PS, should guide the AOI selection.

3.3 Best path selection

As a first step, the image perpendicular baselines and dates of acquisition are analysed to find the best connection strategy. Several options are possible:

- 1) the standard procedure is to select one master image for all the subsequent processing. The default choice is the acquisition closer to the “mass center” of the point cloud representing the various images in the (B_r, B_\perp) space, but any other image can be chosen by the user.
- 2) Alternatively, a “best path” connecting all the images can be selected, based on a minimum spanning tree obtained by an ad hoc distance function, as detailed in [18]. This approach can ease the sub-

sequent co-registration procedure and enable a more accurate amplitude equalization operation (described in the following), thus increasing the number of detected PS; in particular, use of the stepwise approach often allows inclusion in the processing chain of acquisitions which would be excluded from the standard “single master” approach, due to the low coherence caused by their very large temporal and/or spatial baselines [19].

3.4 Co-registration

Once the structure of the InSAR pairs tree is defined, the images are co-registered by computing cross-correlations between a high number of image patches. Patch coordinates and dimensions can be generated by default as a regular pattern or specified by the user. Fractional shifts are computed for each patch. A preliminary coarse co-registration step is followed by a finer, sub-pixel co-registration procedure.

3.5 Resampling

Based on the results of the preceding step, a polynomial warp function is applied to each of the SAR images. Resampling is done onto the chosen master image, either directly, or through the stepwise approach described in sect. 3.3. User-defined oversampling factors can be adopted, and a specifically-designed inter-

polator kernel function is applied [17].

3.6 Amplitude equalization

To ensure homogeneous weighting of all the acquisitions in the subsequent steps, image amplitudes need to be equalized at least in a relative way. For this, a particular procedure is adopted which exploits targets with high amplitude inverse coefficient of variation (ICV), defined as the ratio of the SAR amplitude and its standard deviation, computed on each pixel along the temporal axis: the full absolute calibration procedure is applied only to the master image, and then all other images in the stack are relatively corrected for both system- and geometry-related calibration factors [23]. The calibrated amplitude image stack is a side-product, which can be useful for other applications.

3.7 Differential interferogram generation

Standard DInSAR processing is performed on the co-registered image pairs, including interferometric phase computation, topographic phase simulation and subtraction. At the end of this step, the data stack consisting of interferometric differential phase fields is also available as a second intermediate product.

3.8 Amplitude stability map evaluation

PSCs are detected by thresholding their ICV value. Threshold values are assigned through considerations about the assumed system noise, which in turn is a function of the number of available images, the sensor noise floor, etc.

3.9 Phase Unwrapping

Phase unwrapping is required in order to infer absolute values of the differential phase evaluated on the PSC locations. Two procedures are available: a sparse-grid Minimum Cost Flow and a more ad hoc procedure, described in detail in [24] and [25].

3.10 Atmospheric phase filtering

Low-order polynomial fit and de-trending operations are performed on the phases of the detected PSCs, in order to obtain a first estimate of the APS component. Further refinements in the APS estimation are performed later in the iterative process.

3.11 DEM error & movement estimation

DEM error phase components are directly proportional to the perpendicular baseline. Terrain motion can often be assumed to be a continuous function of time, and so gives rise to a phase contribution which is “smooth” as a function of the temporal baseline. Exceptions to the latter rule must of course be taken into account occasionally, when analyzing particular measurement

points. A fit and de-trending procedure analogous to that necessary for the APS estimation is performed in the temporal and spatial baseline domain. As a result, the DEM error and movement of each PS pixel is estimated and removed. The two preceding steps are performed first on a limited number of low-baseline images, then are iterated several times, each time including more images and more pixels within each image. In this way, improvements in the estimation and subtraction of the APS and the other components propagate to the whole image stack, allowing the detection of more PS pixels, until convergence is reached.

A measure of reliability of each PS point is the inter-image coherence, defined as $\gamma = \frac{1}{N} \sum_k |\exp j(\phi_k - \phi_{\text{model}})|$, i.e. the sum over the N images of the residual between actual and modelled phase trends. The model phase is the sum of all the contributions due to APS, DEM error, and displacement.

The same task can be attempted in the framework of the general technique of Blind Source Separation, through application of the algorithm of Independent Component Analysis [26]. The main advantage of this approach is that no a priori hypotheses are required concerning the deformation model. However, the results can be strongly affected by unwrapping errors along the temporal/spatial baselines.

3.12 Geocoding

By using the DEM error estimated in the preceding step, precise height information about each PS can be retrieved. This can be used again iteratively to improve the horizontal positioning. High accuracies can be reached both in Lat/Long position and in height.

3.13 Output

The SPINUA output products are described in the following.

Multi-Image SAR reflectivity map: this is the full-resolution SAR amplitude map obtained by the incoherent averaging of all the input SAR acquisitions. Its high resolution and low levels of speckle noise, coupled to the high sensitivity of SAR data to surface texture, make it a useful investigation tool for subtle morphological features of the study area.

APS maps: the independent APS contributions – one for each processed SAR acquisition – can be studied for atmospheric applications.

PS Maps in both SAR and WGS84 coordinates: the detected PS coordinates are provided in tabular form both in the original master SAR reference, and in the DEM geographic coordinate system (WGS84).

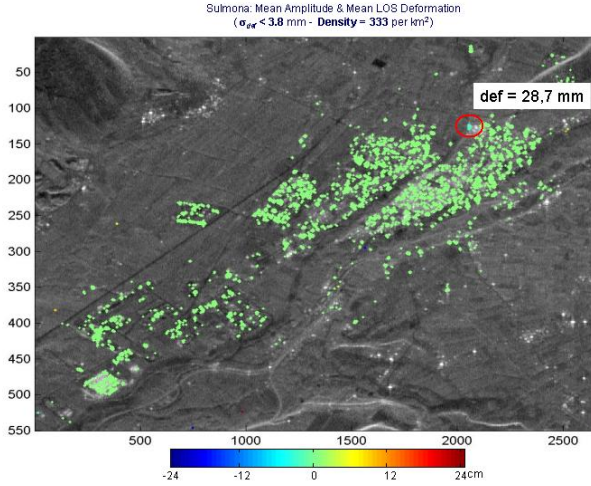


Fig. 2. PS velocity map over the city of Sulmona (Central Italy): the dominant green color indicates stability of the area. The red circle highlights an isolated subsidence area, with displacement rate of about 3 cm in 5 years. The backdrop is the multi-image amplitude SAR reflectivity map.

PS LOS height time series: the temporal series of height variations for each of the final PS (one measurement for each processed SAR acquisition) are provided. A time series represents the component of displacement parallel to the line of sight (LOS).

DEM corrected at PS locations: the height of the input DEM is corrected for the errors computed at the PS locations, through the SPINUA technique. A new DEM can thus be generated, with spot heights at PS having improved precision.

All these algorithms are designed in a fully parametrical way, and are thus easily adaptable to ingest data from different sensors. The steps up to the standard DInSAR processing are performed with a slightly modified version of the DORIS free DInSAR software package [27]. The subsequent operations are performed by specifically developed software. An interactive module is available to select a point on the raster multi-image reflectivity map, perform the APS, DEM error and deformation phase contributions estimation and subtraction, and display the results. The pixel inter-image coherence value is also provided after evaluation and subtraction of each signal component. This helps in understanding the reliability of the detected phase trends. It is particularly useful in the case of low density of PS, where assessment and validation of processing results can be critical.

4. RESULTS AND CONCLUSIONS

Figs. 2, 3, and 4 show some results of application of the SPINUA technique to a landslide dataset on Central Italy. Fig. 2 shows a PS map over the city of Sulmona, used as a validation test site for the SPINUA approach.

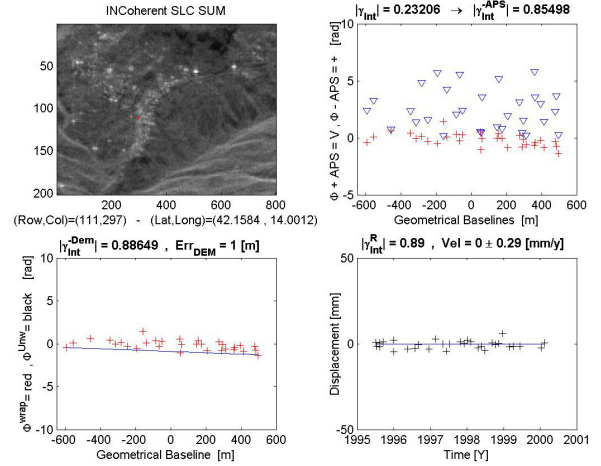


Fig. 3. Caramanico Test Site: sample results of an interactive stable persistent point analysis.

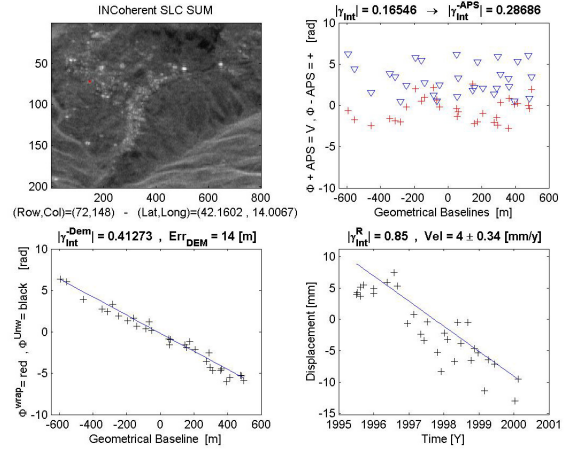


Fig. 4. Caramanico Test Site: movement analysis on a persistent point.

PS pixels are represented by colored points superposed to the multi-temporal SAR reflectivity map. The PS color scale is proportional to the average movement detected on each point. A small area exhibiting a downward total displacement of 28.7 mm over 5 years is highlighted by a red circle. In situ investigations are in due course to verify the nature of this displacement.

Figs. 3 and 4 show two examples of the interactive processing results over the landslide site of Caramanico Terme (Italian Central Apennines). The first one refers to a stable point, the second one exhibits an average downward linear displacement of about 4 mm/year. Displacement rates detected on the Caramanico area agree qualitatively with in situ measurements and models of the landsliding processes, carried out by geologists and other collaborators in the framework of several projects related to the test site.

Results are also being validated on other landslide test sites, in the framework of different projects. As men-

tioned, the SPINUA processing chain is being maintained and constantly developed and upgraded in order to improve its performances and to widen its fields of application, for what concerns both the test site characteristics, and the SAR data.

ACKNOWLEDGEMENTS

This work is partly supported by the LEWIS EU project. (EVGI-CT-2001-00055).

REFERENCES

- [1] Fruneau, B., Achache, J., Delacourt, C. "Observation and Modelling of the Saint-Etienne-de-Tinée Landslide Using SAR Interferometry", *Tectonophysics* 265: 181-190, 1996.
- [2] Rott H., Scheuchl, B., Siegel, A., Grasmann, B. "Monitoring very slow slope movements by means of SAR interferometry: a case study from a mass waste above a reservoir in the Ötztal Alps, Austria". *Geoph. Res. Letters* 26: 1629-1632, 1999.
- [3] J. Wasowski, F. Bovenga, R. Nutricato, A. Refice and D. Casarano, "Test of Applicability of Multitemporal Differential Interferometry Analysis to Landslide Investigations in Peri-Urban Areas", *Proc. FRINGE'03*, ESA-ESRIN, Frascati, Italy, 1-5 December, 2003.
- [4] Refice, A., Guerriero, L., Bovenga, F., Wasowski, J., Veneziani, N., Atzori, S., Ferrari, A. R., Marsella, M. (2000). "Detecting Landslide Activity by SAR Interferometry", *Proc. ESA ERS-ENVISAT Symposium*, Gothenburg, Sweden, 16-20 October 2000.
- [5] Refice, F. Bovenga, J. Wasowski, L. Guerriero, "DInSAR applications to landslide studies", *Proc. IGARSS 2001*, Sydney, Australia, 09-13 July 2001.
- [6] J. Wasowski, A. Refice, F. Bovenga and R. Nutricato, "On the Applicability of SAR Interferometry Techniques to the Detection of Slope Deformations", *Proc. 9th IAEG Congress*, Durban, South Africa, 16-20 September 2002.
- [7] A. Ferretti, C. Prati, F. Rocca, "Permanent Scatterers in SAR Interferometry", *IEEE Trans. Geosci. Rem. Sens.*, Vol.39, No.1, pp. 8-20, Jan. 2001.
- [8] P. Berardino, G. Fornaro, R. Lanari, E. Sansosti, "A new Algorithm for Surface Deformation Monitoring Based on Small Baseline Differential SAR Interferograms", *IEEE Trans. Geosci. Rem. Sens.*, Vol. 40, No.11, pp. 2375-2383, Nov. 2002.
- [9] O. Mora, J.J. Mallorqui, A. Broquetas, "Linear and nonlinear terrain deformation maps from a reduced set of interferometric sar images", *IEEE Trans. Geosci. Rem. Sens.*, Vol. 41 No. 10, pp. 2243-2253, Oct. 2003.
- [10] S. Usai "A Least-Square Approach for Long-term Monitoring of Deformations with Differential SAR Interferometry", *Proc. IGARSS 2002*, Toronto, Canada, June 24-28, 2002.
- [11] R. F. Hanssen, *Radar Interferometry: Data Interpretation and Error Analysis*, Kluwer Academic Publishers, Dordrecht, 2001.
- [12] P. Berardino, G. Fornaro, R. Lanari, M. Manunta, M. Manzo, A. Pepe, E. Sansosti, "A Two-Scale Differential SAR Interferometry Approach for Investigating Earth Surface Deformation", *Proc. IGARSS 2003*, Toulouse, France, July 21-25 2003.
- [13] A. Ferretti, C. Prati, F. Rocca, "Nonlinear subsidence rate estimation using permanent scatterers in differential SAR interferometry", *IEEE Trans. Geosci. Rem. Sens.*, Vol. 38, No.5, pp. 2202-2212, Sept. 2000.
- [14] F. Rocca, "3D motion recovery from multiangle and/or left right interferometry", *Proc. FRINGE'03*, ESA-ESRIN, Frascati, Italy, 1-5 December, 2003.
- [15] A. Ferretti, C. Colesanti, D. Perissin, C. Prati, F. Rocca, "Evaluating the effect of the observation time on the distribution of SAR Permanent Scatterers", *Proc. FRINGE'03*, ESA-ESRIN, Frascati, Italy, 1-5 December, 2003.
- [16] A. Refice, F. Mattia, G. De Carolis, "Polarimetric Optimisation applied to permanent scatterers identification", *Proc. IGARSS 2003*, Toulouse, France, 21-25 July 2003.
- [17] R. Nutricato, F. Bovenga, A. Refice, "Optimum Interpolation and Resampling for PSC Identification", *Proc. IGARSS 2002*, Toronto, Canada, June 24-28 2002.
- [18] A. Refice, F. Bovenga, R. Nutricato, "Stepwise Approach to InSAR Processing of Multitemporal Datasets", *Proc. FRINGE'03*, ESA-ESRIN, Frascati, Italy, 1-5 December, 2003.
- [19] A. Refice, F. Bovenga, R. Nutricato, M.T. Chiaradia, "Assessment of Multitemporal DInSAR Stepwise Processing", to appear in *Proc. IGARSS 2004*, Anchorage, Alaska, September 20-24 2004.
- [20] S.D.P. Williams, Y. Bock and P. Fang, "Integrated satellite interferometry: Tropospheric noise, GPS estimates and implications for interferometric synthetic aperture radar products", *J. Geophys. Res.*, 103: 27051-27067, 1998.
- [21] R. F. Hanssen, T. M. Weckwerth, H. A. Zebker, and R. Klees, "High-resolution water vapor mapping from interferometric radar measurements", *Science*, 283:1295-1297, February-26, 1999.
- [22] J. Muñoz Sabater, R. Hanssen, B.M. Kampes, A. Fusco and N. Adam, "Physical Analysis of Atmospheric Delay Signal Observed in Stacked Radar Interferometric Data", *Proc. IGARSS'03*, Toulouse, France, July 21-25, 2003.
- [23] F. Bovenga, A. Refice, R. Nutricato, G. Pasquariello, G. De Carolis, "Automated Calibration of Multi-Temporal ERS SAR Data", *Proc. IGARSS 2002*, Toronto, Canada, June 24-28 2002.
- [24] A. Refice, F. Bovenga, S. Stramaglia, D. Conte, "Use of scaling information for stochastic atmospheric absolute phase screen retrieval", *Proc. IGARSS 2002*, Toronto, Canada, June 24-28 2002.
- [25] F. Bovenga, A. Refice, S. Stramaglia, D. Conte, "Phase Unwrapping by means of scaling information and global optimization algorithms", *Proc. 9th International Symposium on Remote Sensing*, Agia Pelagia, Crete, 22-27 September 2002.
- [26] F. Bovenga, S. Stramaglia, R. Nutricato, A. Refice, "Discrimination of different sources of signals in Permanent Scatterers technique by means of Independent Component Analysis", *Proc. IGARSS 2003*, Toulouse, France, July 21-25 2003.
- [27] B. Kampes, R. Hanssen, Z. Perski, "Radar Interferometry with Public Domain Tools", *Proc. FRINGE'03*, ESA-ESRIN, Frascati, Italy, 1-5 December, 2003.